Passive Millimeter-Wave Ranging Using Discrete Lenses with Wave-Front Coding

Joseph A. Hagerty and Zoya Popović *

Department of Electrical and Computer Engineering,
University of Colorado, Boulder CO 80309-0425 USA

*On leave from the University of Colorado at the
Technische Universität München, Lehrstuhl für Hochfrequenztechnik
Arcisstraße 21, D-80333 München, Deutschland

Email: popovic@hft.ei.tum.DE, hagertyj@colorado.EDU

***Abstract*— This paper presents an approach to millimeter-wave passive ranging using a method that has been demonstrated in the visible range. Ranging is achieved for multiple objects by way of a receiving discrete lens with modulated amplitude and/or phase response. The result is a set of image patterns with orthogonally coded, range dependent spatial frequency content. We present simulations on a relatively small (100-element) discrete lens antenna array with a cosinusoidal amplitude mask and half-wavelength period at 94 GHz. The feasibility of the approach along with comparisons to the optical counterpart are discussed.**

I. Introduction

Millimeter-wave ranging is of interest since most metal objects have high black-body emission in this range and there is also a low-attenuation window in the atmosphere absorption curve around 94 GHz. Waves in this frequency range penetrate through dust, fog and smoke and are therefore of interest to the military. Some ranging systems around 90 GHz have been demonstrated, primarily by TRW, but they involve transmission and are therefore easily detectable. A review of passive millimeter-wave ranging is presented in [1].

In the optical domain, a number of different ranging techniques are used. Recently, a technique referred to as *wave-front coding* was implemented for microscopy applications [2]. A standard lens images an object situated on the optical axis onto a focal point. If however a mask is used in front of the lens, as shown in Fig. 1, the range can be determined theoretically from the magnitude of the transfer function obtained by convolution of the phase front with the pupil function of the aperture. In the optical system the image is sampled with a CCD array and the spatial frequency content of the image is Fourier-analyzed using digital signal processing. The Fourier transform of the image will contain peaks that move out to the higher-order spatial modes as the range of the object increases. Peaks in measured spatial frequency are then correlated with a calculated magnitude of the transfer function in order to calibrate the range of the object.

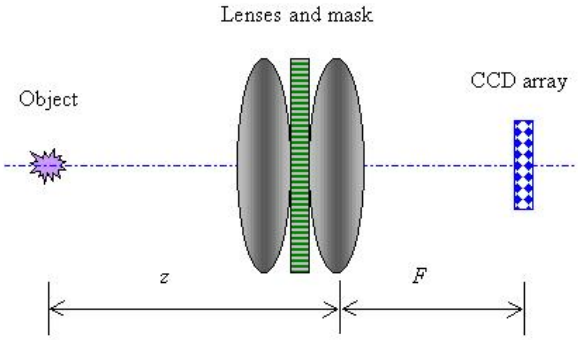

Fig. 1. Schematic of an optical ranging system with wave-front coding. The phase-amplitude mask changes the transfer function of the system. The Fourier transform of the image will contain peaks that move out to the higher-order spatial modes as the range of the object increases.

II. Millimeter-wave imaging

In this paper, we examine the applicability of this approach to longer wavelengths in the millimeter-wave region, e.g. at 94 GHz. We specifically use a discrete lens (a multi-beam antenna array) that can include the functions of the lens and mask in the optical system from Fig. 1. In addition, the variety of possible masks is much

larger than in an optical system, and there is a possibility of adding gain into the lens as amplifiers in W-band have been demonstrated by a number of groups in the past decade [3], [4], [5]. The millimeter-wave implementation of the optical setup from Fig. 1 includes a lens antenna array in which the delay and gain (and/or attenuation) in each element is modified from a more standard constrained lens to that corresponding to a lens with a mask. This is demonstrated schematically in Fig. 2. At the object side of the

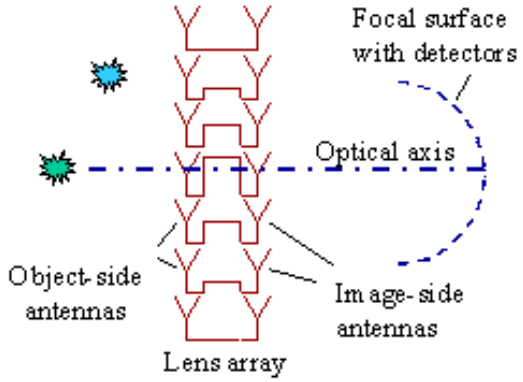

Fig. 2. Schematic of millimeter-wave passive ranging front end (a) and a single element of a discrete lens antenna array (b). The delay and gain (or attenuation) vary between array elements. The variation can be modified for different masking functions.

lens array, each antenna element samples the incident wavefront. Since the antennas are spaced by a half free-space wavelength, the sampling of the wavefront at bore-sight (direction of the optical axis) is Nyquist sampling. Each element introduces a delay and possibly an amplitude change before being re-radiated by the image-side antennas.

Instead of a CCD array in this configuration, an array of antennas with detectors is placed on an imaging surface. The detectors can be designed to under-sample, Nyquist-sample or over-sample the image, depending on other requirements. Details on previous work in lens antenna arrays at X through Ka-bands (10 to 30 GHz) relevant to this work can be found in [6], [7], [8].

III. Ranging with a wave-front encoded image

In order to gain some insight into the applicability of wave-front coding to millimeter-wave ranging, a very small 94 GHz array was simulated using an in-house developed electromagnetic simulator used also in [7]. The array is small compared to a directly scaled version of the optical system, which would be on the order of 10,000 free-space wavelengths across and would make it impractical to implement (30 m diameter). Here, the modeled array is 5 free-

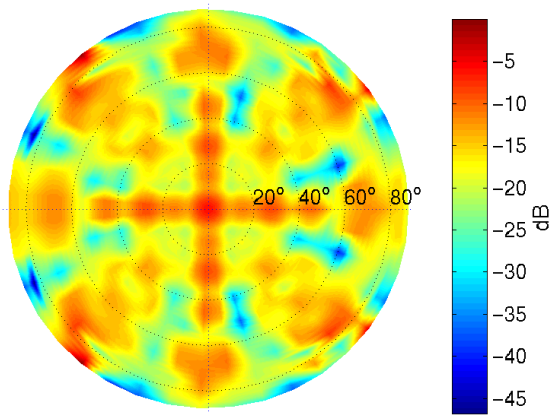

Fig. 3. Simulation of images sampled by detectors positioned over the image surface of a 100-element lens with bore-sight object at 6 (a) and 10 (b) free-space wavelengths from a masked lens with half-wavelength period.

space wavelengths across (100 elements, about 2 cm in diameter), and the antenna elements are assumed to be low-gain with half-wavelength spacing. The mask is a simple cosine amplitude mask, similar to the one used in the optical system. The image surface is sampled by simulated detectors for varying object distance.

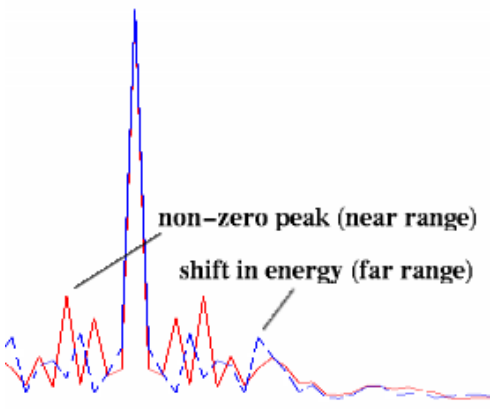

Fig. 4. Fourier transforms of axial slices from the image patterns of Fig. 3. The shift in energy outward from the main peak (the zero-frequency peak) along the spatial frequency axis indicates an increase in range.

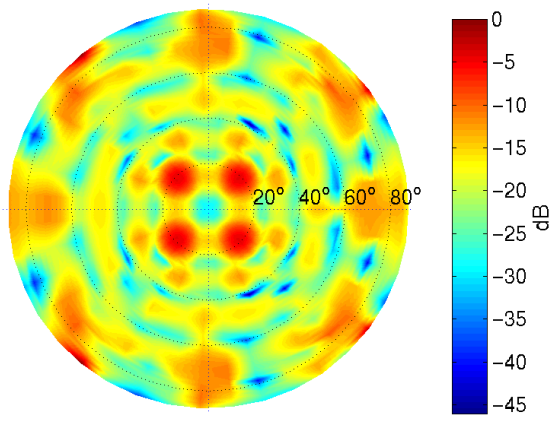

Fig. 5. Simulation of image sampled by detectors positioned over the image surface of a 100-element lens with bore-sight object at 30 free-space wavelengths from a masked lens with half-wavelength period.

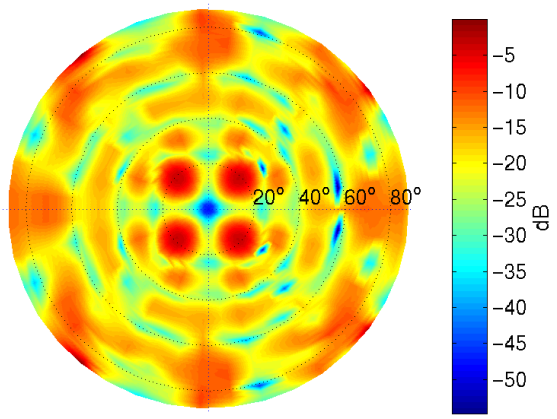

Fig. 6. Simulation of image sampled by detectors positioned over the image surface of a 100-element lens with bore-sight object at 100 free-space wavelengths from a masked lens with half-wavelength period.

The ranging process is demonstrated for on-axis objects located 6λ and 10λ from the lens. The Fourier transform of axial slices from each image of Fig. 3 are given in Fig. 4 showing an expected peak at the zero spatial frequency, and additional peaks at higher order spatial modes. A mathematical analysis shows that the energy in these modes shifts to higher frequencies as the range of the object increases. This is demonstrated in Fig. 4 where the expected shift in spatial frequency of the image is clearly shown. In a working system, a calibration for the range is straightforward since the amount of frequency shift of a given peak is linear with the change in range. The same Fourier analysis can be done on the image patterns given for additional object distances shown in Figs. 5 and 6 where the object is progressed further from the lens.

In Figs. 3-6 the object is kept at bore-sight while the range is increased. When the object is located at some angle with respect to the optical axis, the range on the image surface also shifts. The image of Fig. 7 visually demonstrates the effects of the aberrations which become more pronounced as objects move off-axis.

IV. Discussion

In summary, this paper presents simulations of a passive millimeter-wave ranging front end that uses wave-front coding to determine the range. Compared to the implementation in the optical region of the spectrum, there are several benefits to using this technique at millimeter wavelengths. In the optical implementation, the aperture efficiency suffers because roughly half of the mask is dark (absorptive), and the number of possible masks is limited. In the millimeter-wave region, the lens can be designed to have variable amplitude by using gain elements (amplifiers); but in principle, a pure phase mask with practically any phase variation can be coded into the delay lines of the discrete lens array. It should be noted, however, that a mask different from the cosine mask presented here can require a significantly different interpretation (and mathematical analysis) of the transfer functions of the images [9], [2].

The practicality of this technique depends on the required range and range resolution The useful range is given by the size of the lens, so large lenses would be needed for large range requirements. The resolution depends on a number of factors, such as element spacing in the lens and detector spacing on the image plane. For example, the image pattern of Fig. 8 shows the effects

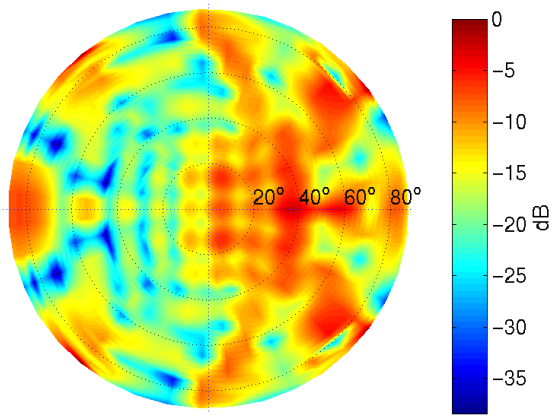

Fig. 7. Simulation of image sampled by detectors positioned over the image surface of a 100-element lens with bore-sight object at 10 free-space wavelengths 20° off-axis from a masked lens with half-wavelength period.

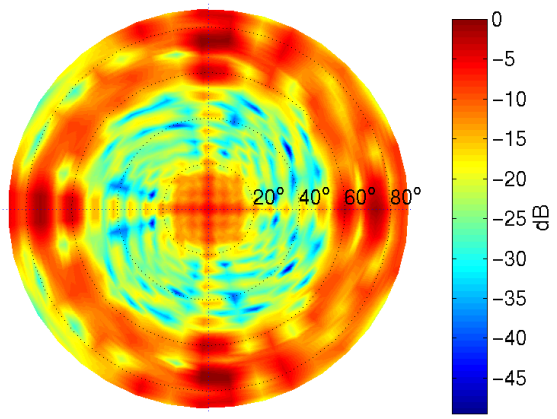

Fig. 8. Simulation of image sampled by detectors positioned over the image surface of a 100-element lens with bore-sight object at 30 free-space wavelengths 20° off-axis from a masked lens with half-wavelength period.

of increasing the lens aperture size without increasing the number of elements (i.e. increasing the array spacing to a full-wavelength). Most of the information in the image for half-wavelength spacing is contained within the 40° boundary and within the 20° boundary for one-wavelength spacing.

The implementation of the discrete lens at 94 GHz is amenable to photolithographic fabrication and there are a variety of appropriate antenna elements and guiding structures which have been developed in the past two decades that can be applied to this approach [10], [11]. Possible detector arrays for sampling the image are Schottky diodes and bolometers [12], [13].

V. Acknowledgments

The authors would like to thank Prof. W. T. Cathey at the University of Colorado, Boulder for many helpful discussions, and Dr. J. Vian, now at MIT Lincoln Labs, for help with the simulations. This work was funded by the Office of the Secretary of Defense and the Office of Naval Research under a MURI program on RF Photonics N00014-97-1-1006 and the Army Research Office under a MURI program on Quasi-Optical Power Combining DAAH04-98-1-0001.

References

[1] R. W. Hardin, "Passive millimeter wave technology keeps the skies safe," *The International Society for Optical Engineering Magazine*, Apr. 2000.

[2] G.E. Johnson, E.R. Dowski, and W.T. Cathey, "Passive ranging through wave-front coding: information and application," *Applied Optics*, vol. 39, no. 11, pp. 1700–1710, Apr. 2000.

[3] A. Werthof, T. Gravem, and W. Kellner, "W-band amplifier fabricated by optical stepper lithography," *IEEE MTT-S Int. Microwave Symp. Dig.*, pp. 689–692, June 1999.

[4] Y. C. Leong and S. Weinreb, "Full W-band MMIC medium power amplifier," *IEEE MTT-S Int. Microwave Symp. Dig.*, pp. 951–954, June 2000.

[5] D. L. Ingram, Y. C. Chen, I. Stones, B. Brunner, P. Huang, M. Biedenbender, J. Elliott, R. Lai, D. C. Streit, K. F. Lau, and H. C. Yen, "Compact W-band solid-state MMIC high power sources," *IEEE MTT-S Int. Microwave Symp. Dig.*, pp. 955–958, June 2000.

[6] Z. Popović and A. Mortazawi, "Quasi-optical transmit/receive arrays," *IEEE Trans. Microwave Theory Tech.*, vol. 45, no. 10, pp. 1964–1975, Oct. 1998.

[7] J. Vian and Z. Popović, "Smart lens antenna arrays," *IEEE MTT-S Int. Microwave Symp. Dig.*, pp. 129–132, 2001.

[8] M. A. Forman, J. Vian, and Z. Popović, "A K-band full-duplex transmit-recieve lens array," *IEEE MTT-S Int. Microwave Symp. Dig.*, pp. 1831–34, 2001.

[9] K.H. Brenner, A.W. Lohmann, and J. Ojeda-Castaneda, "The ambiguity function as a polar display of the OTF," *Optics Comminications*, vol. 44, no. 5, pp. 323–326, Oct. 1982.

[10] G. P. Gauthier, J. P. Raskin, and L. P. B. Katehi et al., "A 94 GHz micromachined microstrip antenna," *IEEE Trans. Ant. and Prop.*, vol. 47, pp. 1761–1766, Dec. 1999.

[11] V. M. Lubecke, K. Mizuno, and G. M. Rebeiz, "Micromaching for terahertz technology," *IEEE Trans. Microwave Theory Tech.*, vol. 46, pp. 1821–1831, Nov. 1998.

[12] D. P. Neikirk, W. W. Lam, and D. B. Rutledge, "Far-infrared microbolometer detectors," *International Journal of Infrared Millimeter Waves*, vol. 5, pp. 245–278, 1984.

[13] C. Zah, D. P. Kasilingam, J. S. Smith, D. B. Rutledge, T. Wang, and S. E. Schwartz, "Millimeter-wave monolithic Schottky diode imaging arrays," *International Journal of Infrared Millimeter Waves*, vol. 6, pp. 981–987, 1985.